

Manuscript Number: CARBPOL-D-17-02170

Title: Ulvan-Chitosan Polyelectrolyte Complexes as Matrices for Biom mineralization

Article Type: Research Paper

Keywords: Ulvan, Chitosan, Scaffolds, Enzyme, Biom mineralization, Alkaline Phosphatase

Corresponding Author: Dr. Mamoni Dash, Ph.D.

Corresponding Author's Institution: Ghent University

First Author: Mamoni Dash, Ph.D.

Order of Authors: Mamoni Dash, Ph.D.; Sangram K Samal; Andrea Morelli; Cristina Bartoli; Heidi A Declercq; Timothy E Douglas; Peter Dubruel; Federica Chiellini

Abstract: Polyelectrolyte complexes (PEC) of chitosan and ulvan were fabricated to study ALP mediated formation of apatitic minerals. Scaffolds of the PEC were subjected to alkaline phosphatase (ALP) and successful mineral formation was studied using SEM, Raman and XRD techniques. Investigation of the morphology via SEM shows globular structures of the deposited minerals, which promoted cell attachment, proliferation and extracellular matrix formation. The PEC and their successful calcium phosphate based mineralization offers a greener route of scaffold fabrication towards developing resorbable materials for tissue engineering.

Suggested Reviewers: Håvard J. Haugen
Department of Biomaterials, University of Oslo
h.j.haugen@odont.uio.no
Prof. Haugen is related to the field of biomaterials.

Antonella Motta
Dipartimento di Ingegneria Industriale , University Trento
antonella.motta@unitn.it
Prof. Motta is renowned for working on cell material interaction on carbohydrates.

Jayakumar Rajadas
Biomaterials and Advanced Drug Delivery Laboratory, Stanford University
jayaraja@stanford.edu
Prof. Rajadas is related to the field of Biomaterials.



Dr. Mamoni Dash
School of Biological Sciences
NISER, Odisha, India

India, 27-06-2017

Dear Editor,

Carbohydrate Polymers

We are honored to submit our manuscript entitled "Ulvan-Chitosan Polyelectrolyte Complexes as Matrices for Biomineralization" for your consideration.

The article focuses on the development of bioresorbable scaffolds for tissue engineering purposes, where the aim was to evaluate a combination of the two different types of charged polymers namely ulvan and chitosan, whose presence could be beneficial to each other. This is a sequential study of the already published work on the mineralization of UV crosslinked ulvan methacrylate scaffolds. In this follow-up study the rationale is to evaluate a greener material as compared to our previously published material, ulvan methacrylate since, exposure to UV irradiation in some cases is known to cause significant degradation of materials. The polyelectrolyte complex of ulvan and chitosan is fabricated to act as a bioresorbable template for the enzyme, alkaline phosphatase to allow nucleation and mineral crystal formation.

Carbohydrate Polymers offer its audience an elegant combination of materials and their interaction with cells for various applications. We hope that even this manuscript with its interdisciplinary approach will be interesting laying more insight into our series of publications related to enzymatic mineralization on polymer matrices.

This article is not under consideration elsewhere and is not published on web as well.

We hope the article will meet the high standards of the journal of Carbohydrate Polymers.

With best regards,

Mamoni Dash

Dr. Mamoni Dash
Principal Investigator
DST-SERB Young Scientist
SBS, National Institute of Science Education and Research (NISER)
Jatni, Odisha 752050, India
E-mail: Mamoni.Dash@niser.ac.in, mamonidash@gmail.com

Tel: +91-9178507001

Highlights

- In the present study, it is aimed to investigate the role of enzymatic mineralization on polymeric structures bearing both cationic and anionic groups.
- Polyelectrolyte complexes of ulvan and chitosan are evaluated as matrices for biomimetic mineralization using ALP.
- Successful mineralization by ALP is observed which improved cellular activity.

1 Ulvan-Chitosan Polyelectrolyte Complexes as Matrices for
2 Biomineralization

3

4 Mamoni Dash,^{1,3,*} Sangram K. Samal,^{2,3} Andrea Morelli,⁴ Cristina Bartoli,⁴ Heidi A. Declercq,⁵
5 Timothy E. L. Douglas,⁶ Peter Dubruel,³ and Federica Chiellini⁴

6 ¹School of Biological Sciences, National Institute of Science Education and Research, Jatni, Odisha
7 752050, India.

8 ²Materials Research Centre, Indian Institute of Science, Bangalore- 560 012, India.

9 ³Polymer Chemistry & Biomaterials Research Group, Ghent University, Krijgslaan 281, S4-Bis, B-
10 9000 Ghent, Belgium.

11 ⁴Biolab Research Group, Department of Chemistry & Industrial Chemistry, University of Pisa, UdR
12 INSTM-Pisa, 56124 Pisa - Italy.

13 ⁵Department of Basic Medical Sciences, Tissue Engineering and Biomaterials Group, Ghent
14 University, De Pintelaan 185 (6B3), 9000 Ghent, Belgium.

15 ⁶Nano- and Biophotonics Group, Department of Molecular Bioengineering, Ghent University,
16 Coupure Links 653, 9000 Ghent, Belgium.

17

18 *Correspondence to: Mamoni Dash, National Institute of Science Education and Research

19 E-mail: Mamoni.Dash@niser.ac.in; mamonidash@gmail.com

20

21

22

23

24 **ABSTRACT**

25 Polyelectrolyte complexes (PEC) of chitosan and ulvan were fabricated to study ALP mediated
26 formation of apatitic minerals. Scaffolds of the PEC were subjected to alkaline phosphatase (ALP)
27 and successful mineral formation was studied using SEM, Raman and XRD techniques.
28 Investigation of the morphology via SEM shows globular structures of the deposited minerals,
29 which promoted cell attachment, proliferation and extracellular matrix formation. The PEC and
30 their successful calcium phosphate based mineralization offers a greener route of scaffold
31 fabrication towards developing resorbable materials for tissue engineering.

32 **Keywords:** Ulvan, Chitosan, Scaffolds, Enzyme, Biomineralization, Alkaline Phosphatase

33

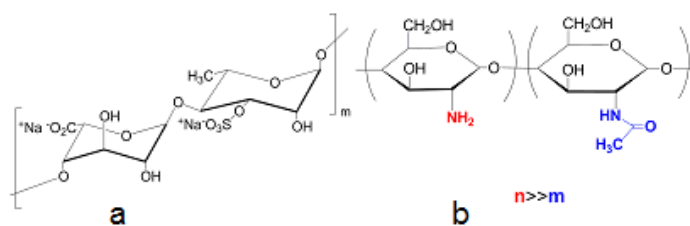
34 **1. INTRODUCTION**

35 Biomimetic mineralization is the process of preparing inorganic crystals in the presence of organic
36 molecules. Biomimetic mineralization attracts interest since it usually leads to crystals with
37 multiscale ordered structures, which are rare in natural minerals. Besides, it is also an easy way to
38 synthesize novel organic/inorganic hybrids. CaCO_3 , BaSO_4 , BaCO_3 , and hydroxyapatite (HAP) are
39 the mostly investigated minerals synthesized via biomimetic mineralization. In the field of
40 biomedical research, polymer scaffolds or hydrogels that mineralized apatite had improved
41 osteoconductivity and osteoinductivity compared to unmineralized polymers (Habibovic & de
42 Groot, 2007). Several polymers have been investigated for this application such as
43 chitosan(Mamoni Dash et al., 2015; Timothy E. L. Douglas et al., 2013; Lišková et al., 2015),
44 ulvan(Mamoni Dash et al., 2014), silk(Samal, Dash, Chiellini, et al., 2014; Samal, Dash, Declercq,
45 et al., 2014), gellan-gum(T. E. L. Douglas et al., 2014), poly(ethylene glycol)(Phadke, Zhang,
46 Hwang, Vecchio, & Varghese, 2010), bacterial cellulose (Zimmermann, LeBlanc, Sheets, Fox, &
47 Gatenholm, 2011), poly(L -lactic acid)(Ruhé et al., 2005) and polycaprolactone(Koupaei &

48 Karkhaneh, 2016). In each case, some type of biological apatite was formed, such as calcium-
49 deficient HAP(Zimmermann et al., 2011), dicalcium phosphate dihydrate (DCPD)(Costa, Dixon, &
50 Rizkalla, 2012), carbonated apatite(Costa et al., 2012),or HAP(Phadke et al., 2010). In this study,
51 polyelectrolyte complexes (PEC) of ulvan and chitosan are evaluated as matrices for biomimetic
52 mineralization. PEC's are mixtures of positively and negatively charged polyelectrolytes blended at
53 the molecular level. Ulvan is an anionic sulphated polysaccharide that is water soluble and semi-
54 crystalline in nature(Mamoni Dash et al., 2014), which can be obtained by extraction from the cell-
55 walls of the green seaweeds belonging to Ulvales (Ulva and Enteromorpha sp.)(Morelli &
56 Chiellini, 2010) The natural availability of ulvan represents a source of abundant and economic
57 renewable resources(Morelli & Chiellini, 2010) with minimal concerns regarding toxicity towards
58 host organisms. Sulfated, rhamnose, xylose, glucuronic and iduronic acids are the main constituents
59 of ulvan (Figure 1)(Mamoni Dash et al., 2014). Ulvan has been reported as anticoagulant,
60 antioxidant, antitumor and immune modulator. Chitosan is a polysaccharide composed of β -(1,4)-2-
61 acetamido-2-deoxy-**d**-glucose and β -(1,4)-2-amino-2- deoxy-**d**-glucose units, is a deacetylated
62 form of chitin(Mamoni Dash, Chiellini, Fernandez, Piras, & Chiellini, 2011; M. Dash, Chiellini,
63 Ottenbrite, & Chiellini, 2011; Mamoni Dash, Piras, & Chiellini, 2009). This natural cationic
64 polymer, offers unique properties; it is biologically renewable, biodegradable, biocompatible, non-
65 antigenic, non-toxic, and biofunctional(Lupascu et al., 2015). Chitosan has been proven to
66 accelerate wound healing, stimulate the macrophage activity, and inhibit the growth of tumor cells
67 and posses antimicrobial properties (R. Muzzarelli et al., 1990; R. A. A. Muzzarelli, 2011). PEC's
68 involve anionic and cationic side chain reactions on their macromolecular backbone (Schwarz,
69 Richau, & Paul, 1991). Therefore, ulvan and chitosan as oppositely charged macromolecules can
70 potentially form a polyelectrolyte assembly.

71 PEC's of ulvan and chitosan are biofunctionalized by employing the natural enzyme alkaline
72 phosphatase (ALP) as mineralization inducer and the osteogenic cell activity of these scaffolds were

73 evaluated. Mineralization and particularly enzymatic mineralization has been a topic of research
 74 interest over the last decade (Timothy E. L. Douglas, Gassling, et al., 2012; Rauner, Meuris, Zoric,
 75 & Tiller, 2017; Saito, Fujii, Soshi, & Tanaka, 2006). A number of investigations have been reported
 76 on matrices like chitosan(M. Dash et al., 2011), fibrin(Timothy E. L. Douglas, Gassling, et al.,
 77 2012) (Gassling et al., 2013) (Timothy E. L. Douglas, Messersmith, et al., 2012), silk(S. K. Samal,
 78 T. Gheysens, & R. Cornelissen, 2014) etc. In the present study, we have aimed to investigate the
 79 role of enzymatic mineralization on polymeric structures bearing both cationic and anionic groups.
 80 In some of our recent works with enzymatic biomineralization, we have studied the behaviour of
 81 both positively and negatively charged polymers individually. Herein, we performed a follow-up
 82 study, where the aim was to evaluate a combination of the two different types of charged polymers,
 83 whose presence could be beneficial to each other. This is a sequential study of the already published
 84 work on the mineralization of UV crosslinked ulvan methacrylate (UMA) scaffolds(Mamoni Dash
 85 et al., 2014) wherein the rationale is to evaluate a greener material as compared to UMA since,
 86 exposure to UV radiation in some cases is known to cause significant degradation of materials. UV
 87 radiation might cause photooxidative degradation, which results in breaking of the polymer chains,
 88 produces free radical and reduces the molecular weight, leading to loss of mechanical properties.
 89 Mineralization includes advantages such as enhancing bioactivity post implantation(Mamoni Dash
 90 et al., 2014; Mamoni Dash et al., 2015), osteoblastic differentiation through increased stiffness
 91 (Olivares-Navarrete et al., 2017) and enhanced binding of growth factors which stimulate bone
 92 healing.(Vo, Kasper, & Mikos, 2012) The evaluation of such matrices could lead to tissue
 93 engineered bioactive bioresorbable scaffolds for bone tissue engineering.



95 Figure 1. The chemical structure representing a) the main disaccharide repeating unit of ulvan, α -L-
96 Iduronic acid (1 \rightarrow 4) α -L-Rha 3S \rightarrow 1(Mamoni Dash et al., 2014) b) chitosan.

97

98 **2. EXPERIMENTAL SECTION**

99 **2.1 Materials.** Ulvan batch in powder as extracted from *Ulva armoricana* was kindly supplied by
100 CEVA within the framework of the EU-funded project BIOPAL. The number average molecular
101 weight of ulvan ($M_n=60000$ g/mol) was determined by using size exclusion chromatography.
102 Pullulan standards (Polymer Laboratories, UK) were used to obtain the calibration curve (range
103 6000-400000 g/mol). Chitosan ($M_w=108$ kDa, $M_w/M_n=2.4$, deacetylation degree (DD)=92% (Piras
104 et al., 2014) was purchased from Sigma–Aldrich, Milan, Italy. Bovine intestinal ALP (specific
105 activity: ≥ 10 DEA units/mg, P7640) and calcium glycerol phosphate (50043) were obtained from
106 Sigma (Sigma Aldrich, Belgium). Ulvan polysaccharide from *Ulva armoricana* was kindly supplied
107 by CEVA ($M_w = 60$ KDa).

108 **2.2 Preparation of Ulvan-Chitosan Polyelectrolyte complexes (UC PEC)** Cylindrically shaped
109 PEC hydrogels containing ulvan (60% w/w) and chitosan (40% w/w) were prepared into a 24-well
110 tissue culture plate. 0.600 mL of ulvan solution in deionized water (30 mg/mL) was added to 0.012
111 mg of chitosan powder contained into each well. Acetic acid 1% (v/v) was poured into each
112 solution to dissolve chitosan powder and the resulting mixture was vigorously stirred until gelation
113 occurred. The hydrogels were left standing at room temperature for 24 hours and then freeze dried
114 under vacuum (0.04 mbar) at -50°C to remove the excess of water.

115 **2.3 Polymer Scaffold Characterization.**

116 **2.3.1 Hydrogel Swelling Degrees**

117 Freeze dried scaffolds (approximately 50 mg) were prepared according to the procedure reported
118 into the previous paragraph and used without any further purifications. The dry PECs were weighed

119 and then immersed in 0.1M PBS (pH 7.4) at room temperature. The samples were weighed at
120 regular time intervals after removal of excess surface liquid by blotting with a soft tissue. The water
121 uptake of the PECs was established by calculating their Swelling Degree % (SD%) as:

122

$$123 \text{ SD\%} = [(W_s - W_d)] / W_d \times 100$$

124 where W_s represents the weight of the swollen sample taken at each time interval and W_d represents
125 the weight of the dry sample taken at the beginning of the experiment. The experiments were
126 performed in triplicate and the SD% reported as the mean value.

127 **2.3.2 FT-IR analysis**

128 FT-IR spectra of the dried scaffolds were recorded as KBr pellets (1/100 mg) in the range 4000–400
129 cm^{-1} by using a Jasco FT-IR 410 spectrophotometer with a resolution of 4cm^{-1} . Each spectrum was
130 recorded after 16 scans.

131

132 **2.3.3 Mineralization of the Scaffolds.** The scaffolds were incubated in a solution of ALP for 30
133 minutes. Three different concentrations of ALP were used in this study (5, 25 and 50 mg/mL). The
134 ALP treated PEC scaffolds of ulvan chitosan will be denoted as UC 5, UC 25 and UC 50
135 respectively. The ALP-soaked scaffolds ($5 \times 5 \text{ mm}^2$ for cell culture and $10 \times 10 \text{ mm}^2$ for mechanical
136 analysis) were subsequently incubated in a mineralization medium (5 mL and 10 mL respectively)
137 containing 0.1 M calcium glycerophosphate (aq) at 37°C . The mineralization medium was refreshed
138 every day. After 7 days of mineralization, scaffolds were rinsed thrice in Milli-Q water to remove
139 residual calcium glycerophosphate and subjected to lyophilization after freezing at -20°C .

140

141 **2.3.4 Scaffold Morphology.** Scanning Electron Microscopy (Hitachi S-3400N) was used to analyze
142 the morphology of the scaffolds. Images were obtained in low vacuum mode (20Pa) to avoid image

143 distortions, using back scattered electrons. Elemental analysis was performed on a Peltier cooled
144 dry EDS system (Thermo Scientific Noran System 7, energy resolution < 125eV).

145

146 **2.3.5 Study of Scaffold Mass Increase.** The mass increase of the scaffolds at different time points
147 after the incubation in calcium glycerophosphate was calculated using previously established
148 equation:

149
$$\text{Mass increase (\%)} = (m_t - m_0)/m_0 * 100$$

150 Where, m_t = the mass of scaffolds after incubation at time t . m_0 = the original mass of scaffolds
151 before incubation and mineralization.

152 The final mass increase was calculated by using the same formula as above but m_t is the dry mass of
153 the scaffolds after mineralization.

154

155 **2.3.6 Raman Spectroscopy.** Fourier transform Raman (FT-Raman) spectra were performed on a
156 NXR FT-Raman Module. The samples were pressed in a suitable gold coated sample holder and a
157 laser power of 0.35 W was used to collect the scans.(Samal, Dash, Chiellini, Kaplan, & Chiellini,
158 2013) 1500 scans were collected at a resolution of 4 cm^{-1} .

159

160 **2.3.7 Thermal Analysis by Thermogravimetry (TGA).** Thermogravimetric analyses were
161 performed using a TA Instruments Series TA 2950 and results were analyzed using
162 Thermogravimetric Analyzer Software (Universal Analysis 2000). Sample weights of 9-13 mg were
163 used and scanned at $10^\circ\text{C}\cdot\text{min}^{-1}$. A temperature range between 30-900°C under a $60 \text{ mL}\cdot\text{min}^{-1}$ flow
164 rate of nitrogen was used for the analysis(Samal et al., 2013).


165

166 **2.3.8 Crystal Structure Elucidation by X-ray Diffraction (XRD).** XRD technique was used to
167 investigate the crystallographic structure of the samples. X-ray diffractometer with CuK α -radiation
168 (PW 3710, 50 kV, 40 mA) was used. Samples were fixed to a position of 2.5° and scanning the
169 detector between 5° 2 θ and 40° 2 θ with a counting time of 5s/step and step-size of 0.01 °2 θ .

170 **2.3.9 Biological Investigations.**

171 **2.3.9.1 Cell culture and seeding.** Pre-osteoblastic MC3T3-E1 cells were purchased from the
172 American Type Culture Collection (CRL-2593). Cells were maintained and expanded in Alpha
173 Modification Minimum Essential Medium containing 10% fetal bovine serum, 100U/ml penicillin,
174 0.1 mg/ml streptomycin (Invitrogen) in humidified 5% CO₂ at 37° C. Confluent MC3T3 cells at
175 passage 25 were trypsinized (0.25% trypsin-EDTA), centrifuged, re-suspended in culture medium
176 and counted. Subsequently 1·10⁵ cells, initially dispersed in 20 μ l of culture medium, were seeded
177 onto the scaffolds in a 24 well plate. After 3 hours of incubation, 980 μ l culture medium was added
178 to the scaffolds. In order to assess the osteogenic differentiation, 24 hours after cell seeding the
179 scaffolds were incubated in osteogenic medium (culture medium supplemented with 10 mM β -
180 glycerolphosphate and 0.3 mM ascorbic acid). Biological investigations were carried out at days 7
181 and 14 after seeding. The medium was replaced every 48 hours. Cells grown on tissue culture plates
182 were used as control.

183 **2.3.9.2 Alkaline phosphatase (ALP) activity.** Alkaline phosphatase activity ALP was determined
184 in culture using MC3T3-E1 cells grown onto the prepared scaffolds at day 7 according to
185 previously established protocols.(Gazzarri et al., 2013) Briefly, treated scaffolds were washed three
186 times with DPBS, treated with lysis buffer, containing Triton X-100 (0.2%), magnesium chloride (5
187 mM) and trizma base (10 mM) at pH 10, for 15 min at 4° C. Cell lysate was centrifuged for 15 min
188 at 10,000 rpm at 4° C. 20 μ l of supernatant were collected and incubated with p-nitrophenyl
189 phosphate at 37° C for 30 minutes. The reaction was stopped by the addition of 2M NaOH. The
190 absorbance at 405 nm was measured with a UV-vis spectrophotometer. The amount of ALP was

191 calculated against a standard curve and normalized to total protein content.  P activity was
192 expressed as nanomoles (nmol) of p-nitrophenol produced per minute.

193 **2.3.9.3 Total protein.** Cellular protein content was measured with a BCA protein assay kit (Pierce,
194 USA) was used to determine the cellular protein content following a protocol of St-Pierre *et al*(St-
195 Pierre, Gauthier, Lefebvre, & Tabrizian, 2005). Cell lysate was incubated with bicinchoninic acid
196 solution for 2 hours at 37° C and the absorbance were measured at 565 nm in a microplate reader.
197 A standard curve using bovine serum albumin was used to generate a standard curve.

198 **2.3.9.4 Quantification of total collagen production.** Quantification of total collagen produced by
199 cells seeded on scaffolds was carried out at day 7. The detailed protocol has been described by
200 Gazzari *et al.*(Gazzarri et al., 2013) Briefly, medium was removed and samples were were rinsed in
201 DPBS. Scaffolds were then incubated for 1 hour with a solution of Direct Red 80 dye (Sigma)
202 prepared in picric acid (0.1%). Dye excess was removed by washing the samples with 10 mM HCl.
203 Bound stain solution was obtained with the incubation 0.1 N NaOH. The absorbance of the dye was
204 read at 540 nm. Known concentrations of collagen type I, filmed on glass slides, were prepared and
205 used for the standard curve. The films were then fixed and treated as the samples.(Junqueira,
206 Bignolas, & Brentani, 1979)

207 **2.3.9.5 Confocal Laser Scanning Microscopy (CLSM):** CLSM investigation was performed to
208 evaluate the morphology of the osteoblasts grown on scaffolds on day 14 of the culture according to
209 a protocol by Gazzari et al.(Gazzarri et al., 2013). Briefly, scaffolds with cells were fixed for 1 hour
210 in 3.8% paraformaldehyde in PBS and permeabilized with 0.2% Triton X-100 for 10 min. The
211 Nikon Eclipse TE2000 inverted microscope (Nikon) and 60X oil immersion objective was
212 employed for samples investigations. Argon Ion Laser (488 nm emission) and a laser diode (405
213 nm) were used to excite FITC and DAPI fluorophores respectively. Images were captured with
214 Nikon EZ-C1 software applying identical instrumental settings for each sample, and were further

215 processed with the GIMP (GNU Free Software Foundation) image manipulation software and
216 merged with Nikon ACT-2U software.

217 **2.3.9.6 Histological Analysis** After cell culturing, cell/scaffold constructs were rinsed with PBS,
218 fixed with 4% phosphate (10 mM) buffered formaldehyde (pH 6.9) (4°C, 24 h), dehydrated in a
219 graded alcohol series and embedded in paraffin. Sections (5-7 µm) were made and stained with
220 hematoxylin & eosin (H&E) and mounted with mounting medium (Cat.No. 4111E, Richard-Allan
221 Scientific).

222 **Statistical analysis.** Data were obtained from triplicate samples and are presented as mean ±
223 standard deviation. Statistical comparison was performed using one-way analysis of variance
224 (ANOVA), and significance was defined at $p < 0.05$ (*) and $p < 0.001$ (**).

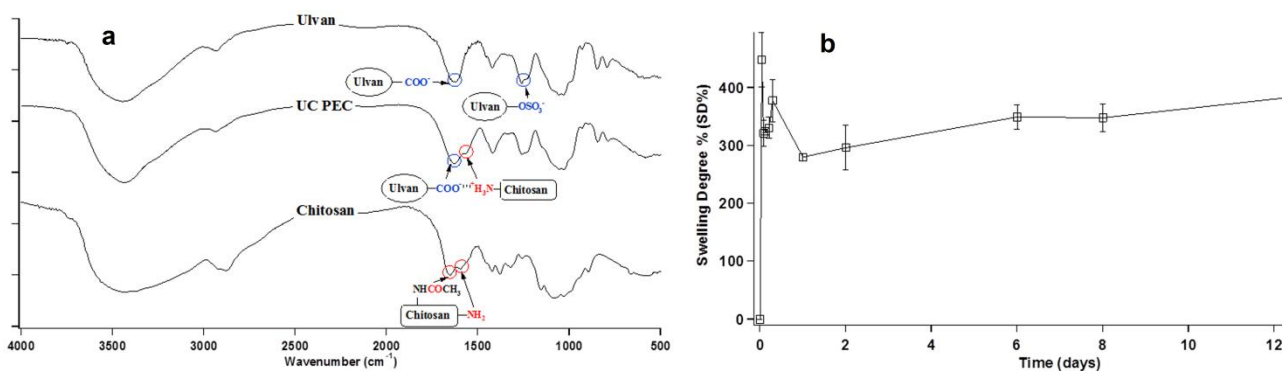
225

226 **3 RESULTS AND DISCUSSION**

227 **3.1 Fabrication of Ulvan-Chitosan PEC**

228 Ulvan represents an anionic polysaccharide containing carboxylates and sulfate esters as negatively
229 charged groups in the repeating disaccharide units (Figure 1). The combination between ulvan and
230 chitosan, as cationic polysaccharide, in mild acidic conditions led to the formation of a
231 polyelectrolyte complex as evidenced by the rapid gelification of the mixture occurring upon
232 vigorous mixing. The PECs were prepared by using ulvan as 60% w/w and chitosan as 40% w/w as
233 optimal feeding composition to theoretically balance the number of positive and negative charges
234 involved in the formation of the complexes and obtain hydrogels stabilized by strong electrostatic
235 forces. FT-IR analysis of UC-PEC confirmed the occurring of electrostatic bonds between the
236 ammonium groups of chitosan and the carboxylate groups of ulvan (Figure 2a).

237



238

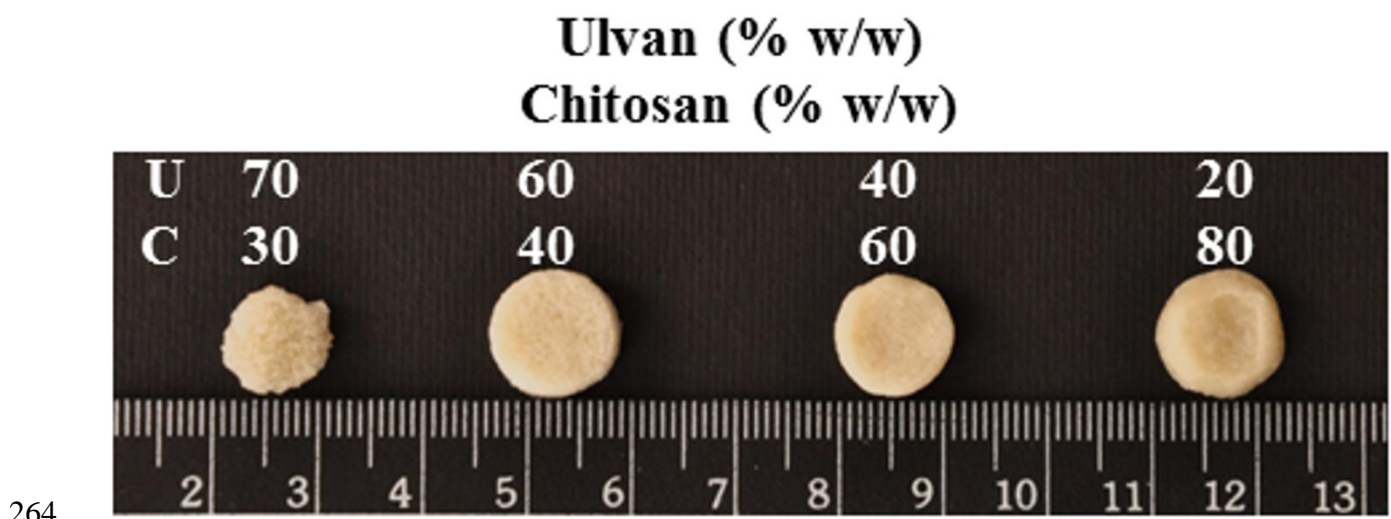
239 Figure 2 a) FT-IR spectra of ulvan, chitosan and UC-PEC b) Swelling degree experiment of UC-
 240 PEC scaffold carried out in PBS solution (0.1M, pH 7.4).

241 The absorption bands relevant to the groups involved in the polyelectrolyte complex formation were
 242 highlighted in blue (ulvan) and red (chitosan). Indeed the absorption bands relevant to the
 243 asymmetrical stretching vibration of carboxylate group of ulvan (1622 cm^{-1}) and the N-H bending
 244 vibration of amine group of chitosan (1596 cm^{-1}) were found shifted in the spectrum of UC-PEC
 245 respectively to 1564 cm^{-1} and 1635 cm^{-1} representing a valid evidence of formation of the
 246 polyelectrolyte complex(Lawrie et al., 2007).

247 The amount of water absorbed by polymeric scaffolds intended to be used in biomedical
 248 applications such as tissue engineering and regenerative medicine represents a crucial parameter
 249 that needs to be evaluated to state their feasibility as successful biomaterials(Slaughter, Khurshid,
 250 Fisher, Khademhosseini, & Peppas, 2009) . The water uptake capability of UC-PEC was evaluated
 251 by swelling experiments in simulated body fluid conditions through the immersion of the dried
 252 scaffolds in PBS solution (0.1M, pH 7.4) for 14 days. The SD% curve showed a maximum value
 253 reached after 1h of immersion followed by a smooth decrease to a constant equilibrium value
 254 reached after 1 day of immersion (Figure 2b). The swelling capability of UC-PEC resulted reduced
 255 to one tenth compared to that reported for ulvan-based hydrogels obtained by UV crosslinking
 256 (Morelli & Chiellini, 2010) due to the neutralization of the negatively charged carboxyl and
 257 sulphate groups of ulvan by the ammonium ions of chitosan. However the SD% values recorded at

258 equilibrium conditions were suitable for supporting the activity of a polymeric scaffold in
259 biomedical applications.

260 As we expected the composition of ulvan (60% w/w) and chitosan (40% w/w) used in the
261 formulation of the PEC provided the most stable scaffolds as evidenced macroscopically by
262 visualizing the shape and the texture of the PECs at different compositions after being immersed in
263 PBS solution (0.1M, pH 7.4) for 14 days (Figure 2c).

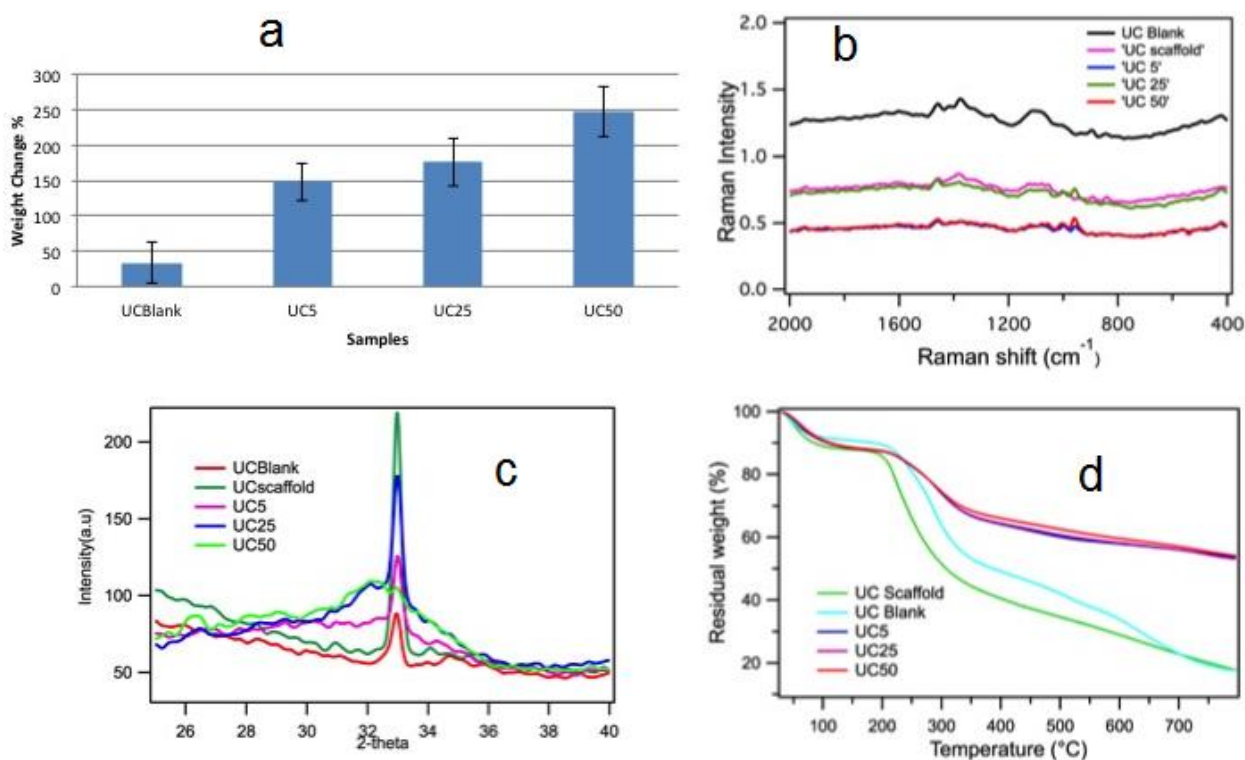


264
265 Figure 2c. UC-PEC scaffolds at different composition after 14 days of immersion in PBS solution
266 (0.1M, pH 7.4). The amount of ulvan and chitosan used for the preparation of the UC-PECs are
267 reported inside the picture as w/w %.

268 3.2 Physical-chemical characterizations of biomineralized PEC scaffolds.

269 The physicochemical characterizations include an indirect measure of the weight increase of the
270 mineralized scaffolds, Raman spectroscopy, TGA. The dry mass percentage is a representation of
271 the ratio of the weight percentage of the scaffolds before and after mineralization as shown in
272 Figure 3a. The dry mass percentage increased upon increasing the ALP concentration from 0 to 50
273 mg mL⁻¹ after 7 days of incubation in calcium phosphate medium. An approximate increase of
274 250% was observed in the UC scaffold weight when treated with 50 mg mL⁻¹ of ALP. The presence

275 of phosphate groups was done through Raman spectroscopy, which revealed a strong peak at 958
 276 cm^{-1} characteristics for the P–O stretching mode (ν_1) of the phosphate group (Figure 3b). The peak
 277 is observed only in samples treated with ALP and is proportional to the to the concentration of the
 278 ALP. The X-ray diffractograms of the mineralized scaffolds also showed a similar trend. (Figure 3
 279 c). A broad reflection peak was seen at $32^\circ 2\theta$ for UC 25 and UC 50 but not for UC 5. The
 280 formations of nano-sized crystals are responsible for the broad peak instead of a sharp peak in
 281 XRD. The thermal property of the mineralized scaffolds was analysed by TGA Figure. 3d). The
 282 scaffolds show a continuous weight loss. In TGA derivative, 1st degradation peak in the
 283 temperature range of 30–130 $^\circ\text{C}$ corresponded to the equilibrium moisture of the samples. The
 284 scaffolds containing ALP possessed mineral, showed higher residue content at 700 $^\circ\text{C}$ (Figure 3d)
 285 and different degradation pattern with an extra shoulder at around 230 $^\circ\text{C}$. This is due to the
 286 presence of minerals compared to unmineralized scaffolds. The amount of residue gave a clear
 287 indication of the presence of the inorganic mineral content in the mineralized scaffolds. There was
 288 no difference in the residue amount with the change in the concentration of ALP.



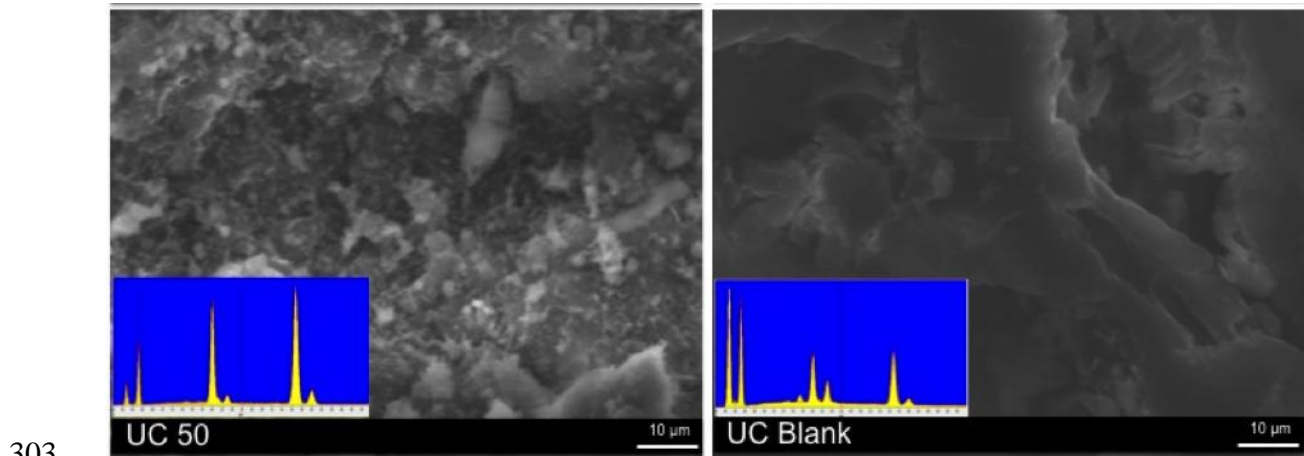
289

290 Figure 3. a) weight change in dry mass after 7 days of mineralization of UC PEC scaffolds b)
 291 Raman spectra of ulvan scaffolds mineralized in the presence of different ALP concentrations, c) X-
 292 ray diffraction patterns of mineralized ulvan scaffolds with different ALP concentrations (the blank
 293 scaffold was unmineralized), d) TGA curves of native and mineralized PEC scaffolds.

294

295 3.3 Morphological Analysis of the mineralized scaffolds

296 The morphology of the mineral deposits in the mineralized PECs was done using SEM (Figure 4)
 297 and their chemical composition was determined using EDS. The blank scaffolds showed only
 298 lamellar structures and no presence of any kind of deposits while the mineralized scaffolds showed
 299 the presence of mineral deposits. Small rounded clustered structures are seen as mineral deposits in
 300 the mineralized scaffolds. The Ca: P ratio in the mineralized scaffolds varied from 1.1 to 1.7 with
 301 increasing enzyme concentration. The blank scaffold also showed a high Ca:P ratio of 1.5 possibly
 302 from the remaining glycerol phosphate solution after washing of the scaffolds.



304 Figure 4. SEM images of UC50 (left) and UC Bank (right).

305 **Table 1:** Atomic percentage of carbon, oxygen, phosphorus and calcium on the UC mineralized
 306 scaffolds

307

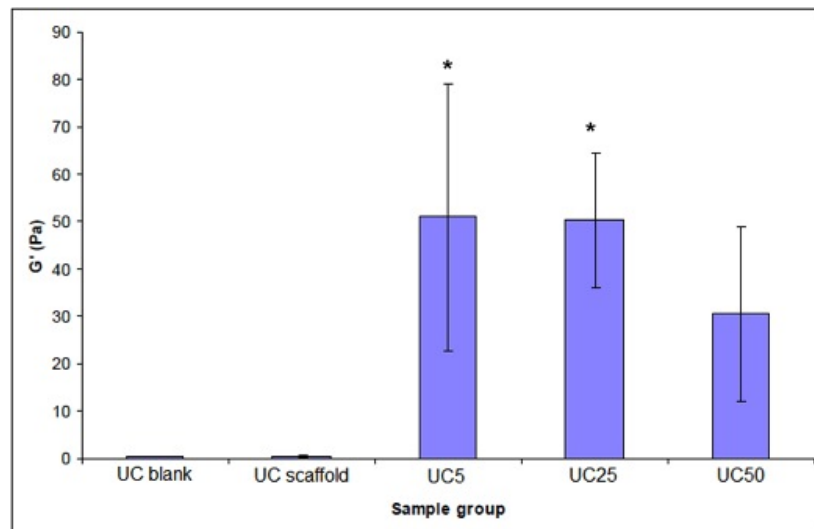
Sample	Calcium (at %)	Oxygen	Phosphorus	Sulfur	Ca:P
--------	----------------	--------	------------	--------	------

308	UC blank	10.7	78.5	7.2	3.6	1.5
309	UC 5	14.9	71.5	13.0	0.6	1.1
310	UC 25	15.4	72.0	12.4	0.2	1.2
311	UC 50	22.7	62.8	13.4	1.1	1.7

312

313 3.4 Mechanical properties of biom mineralized PEC scaffolds

314 The complex moduli of scaffolds mineralized in ALP solutions of different concentrations were
 315 determined using rheology. The results are depicted in Figure 5. The mineralized samples UC 5, UC
 316 25 and UC 50 displayed a significantly higher complex modulus than the ALP-free control (UC
 317 blank) as well the unmineralized PEC scaffold.



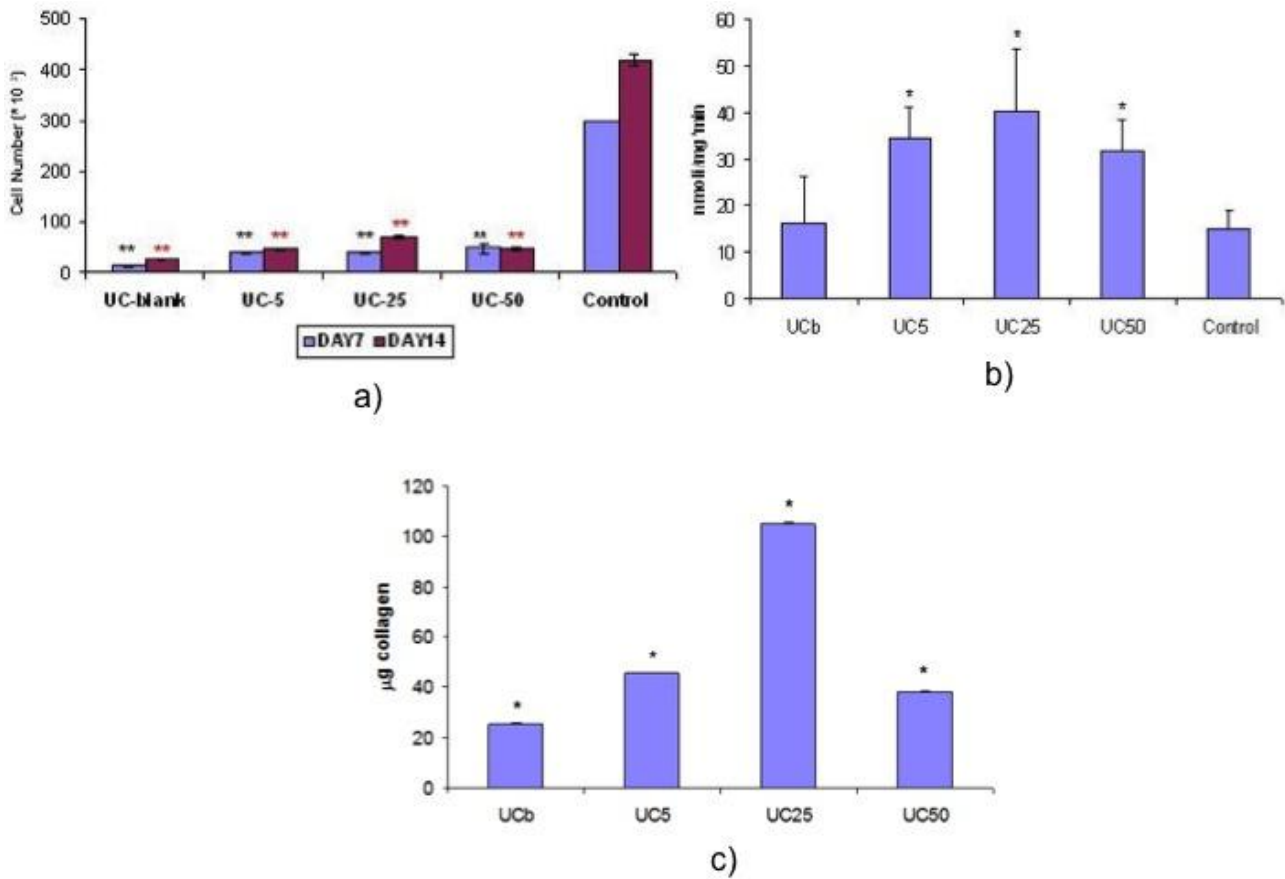
318

319 Figure 5. Rheological measurements of complex modulus of mineralized UC PEC scaffolds, *p <
 320 0.05 relative to UC Blank.

321 3.5 Biological evaluation of the biom mineralized PEC scaffolds

322 The results of cell proliferation of MC3T3-E1 cultured on ulvan-chitosan polyelectrolyte complexes
 323 (UC) are shown in Figure 6a. At day 7 and 14 of culture, enzymatically treated samples showed a

324 cell proliferation significantly higher with respect to the non-enzymatically treated sample (UC
 325 blank) ($p < 0.001$). However, the cell proliferation of MC3T3-E1 on all the typologies of UC
 326 samples resulted significantly lower with respect to the control.



327
 328 Figure 6. a) Cell Proliferation of MC3T3 E-1 cultured UC PEC scaffolds ** (black) Significant at
 329 $p < 0.001$ with respect to control at day 7. ** (red) Significant at $p < 0.001$ with respect to control at
 330 day14=, b) Alkaline phosphatase activity of MC3T3 E-1 cells grown on UC PEC's. * Significant at
 331 $p < 0.05$ with respect to control at day 7, c) Collagen production obtained from MC3T3 E-1 cells
 332 cultured onto UC PEC scaffolds. *Significant at $p < 0.05$ between different samples at day 7.

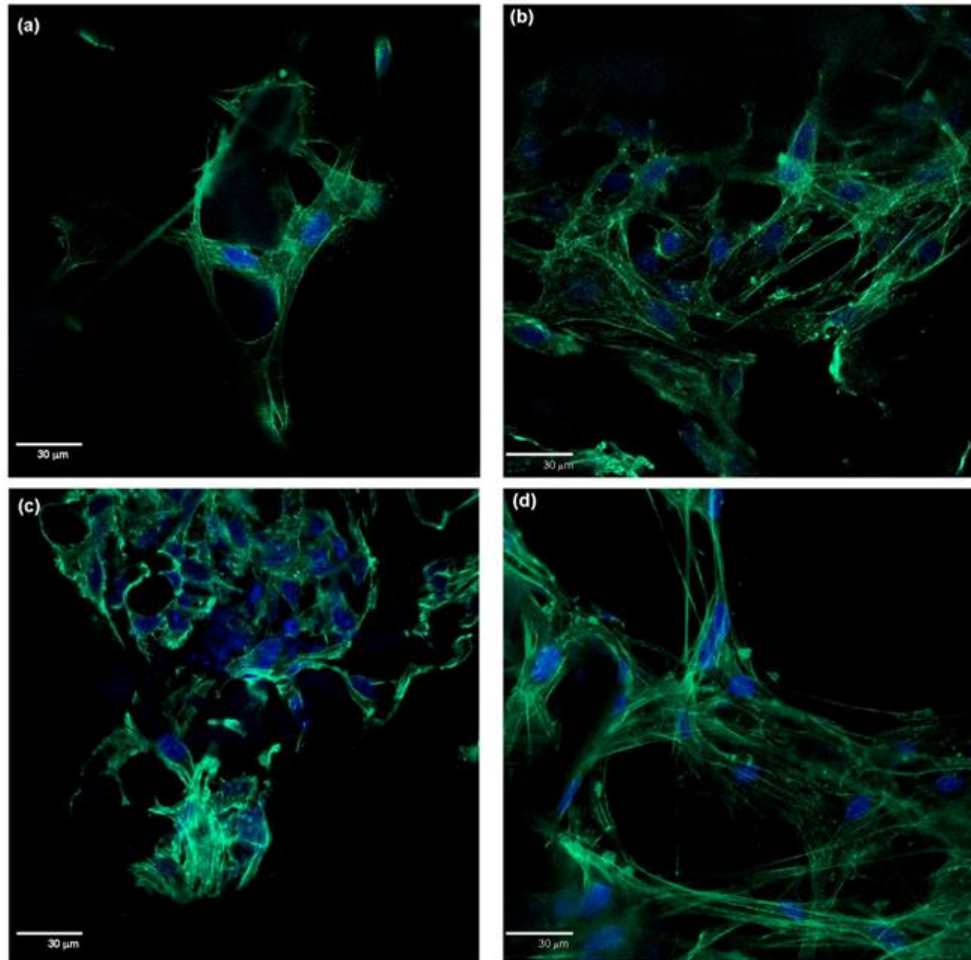
333 The ALP activity of MC3T3-E1 grown on UC PEC scaffolds was monitored at day 7 of culture
 334 (Figure 6b). Cells grown on UC enzymatically treated samples expressed values of ALP activity
 335 significantly higher with respect to the control and to the untreated sample (UCb) ($p < 0.05$),
 336 although the cell number on TCPS was found significantly higher with respect to the UC PEC's.

337

338 The ALP activity indicates an early beginning of the differentiation process towards an osteoblastic
339 phenotype. . The synthesis of a collagen correlates with the expression of osteoblast phenotype in
340 MC3T3-E1 cells (Franceschi & Iyer, 1992). Collagen production by preosteoblast cells cultured on
341 UC PEC was measured and quantified at day 7 of culture. This gives an indication regarding the
342 expression of the osteoblast phenotype. The results highlighted a ~~highlighted~~ a significantly higher
343 collagen production ($p < 0.05$) for cells grown in particular on sample UC 25 (Figure 6 c), although
344 good collagen values were observed for all the enzymatically treated samples in comparison to
345 blank (UC blank).

346 **3.6 Cell morphology investigation by confocal laser scanning microscopy (CLSM)**

347 Confocal laser scanning microscopy was performed at day 7 to investigate the cell adhesion,
348 morphology and cytoskeleton organization. Cells were stained for F-actin and nuclei with FITC-
349 phalloidin and DAPI respectively. Figure 7 shows the morphology and distribution of cells on UC
350 PEC's. In agreement with the cell proliferation results a low number of cells was detected onto non-
351 enzymatically treated sample (UCb). The cells cultured on enzymatically treated UC5 and UC50
352 samples showed an improved adhesion and spreading as confirmed by the presence of fusiform
353 structures well distributed and in contact with each other via cellular extensions (Figure 7b, 7d).
354 Moreover, MC3T3 cells grown on UC25 sample displayed also a cuboidal shape, typical of
355 differentiated osteoblasts (Figure 7c), suggesting its suitability in promoting osteogenic
356 differentiation of pre-osteoblast cells as confirmed by results of ALP activity and collagen
357 production.

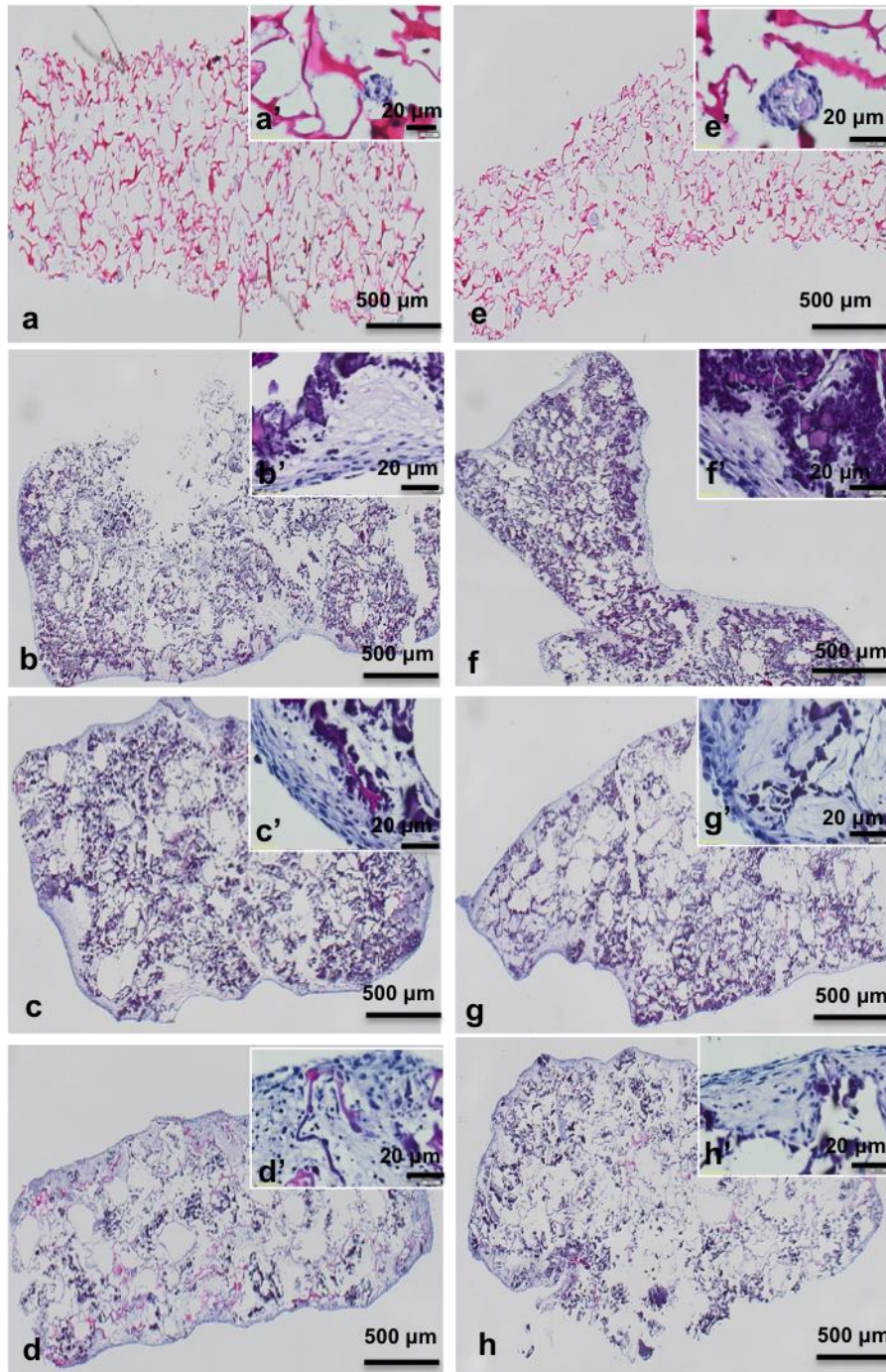


358

359 Figure 7. CLSM micrographs of MC3T3 E-1 cells cultured on UC blank (a), UC5 (b), UC25 (c),
 360 UC50 (d) scaffolds.

361 Cross-sections of cell/scaffold constructs at day 14 and day 21 post-seeding in osteogenic medium
 362 are presented in Figure 8. A dense tissue layer is formed at the edge of the mineralized UC PEC
 363 scaffolds (Fig 10 b, b', c, c', d, d'), in comparison to the blank samples untreated with ALP (fig. 8 a,
 364 a'). after 14 days of culturing. The blank scaffolds (Fig 8 a', e') show the presence of non-attached
 365 clustered cells. Cells cultured on the mineralized scaffolds followed the contours of the scaffolds in
 366 all cases. Cells were able to colonize the edge of the scaffold and formed an extracellular matrix
 367 layer. The size of this adherent tissue layer varies between 40 and 100μm. However, the centers of
 368 the scaffolds were not colonized in this time period. After 21 days of culturing the cell/scaffold

369 constructs, the same trend could be observed as is shown in fig 8 for blank scaffolds (fig 8 e, e) and
370 mineralized scaffolds (fig 8 f, f', g, g', h, h').



371

372 Figure 8. Influence of mineralization on the cell behavior in and the colonization of the scaffolds (
373 ----- 500μm, — 20 μm). Histological analysis (H & E staining) of 3D scaffolds in osteogenic
374 medium at day 14 and day 21 post-seeding. At day 14, a, a') UC blank, b, b') UC 5, c, c') UC 25, d,
375 d') UC 50. At day 21, e, e') UC blank, f, f') UC 5, g, g') UC 25, h, h') UC 50.

376 **4. DISCUSSION** The results described in this work are a comprehensive study on mineralization
377 ability of ALP on PEC of ulvan and chitosan. Traditional mineralization approaches involve
378 alternate soaking of scaffolds in simulated body fluid (SBF) while this study is based on enzyme
379 induced mineralization and is a continuation of our ongoing investigation of mineralization on
380 different polymeric matrices. ALP induced mineralization and the characteristic properties of the
381 materials thereof have been previously investigated on a cationic polymer chitosan, anionic polymer
382 gellan gum, and proteins such as fibrin etc. In this particular study, we investigated a polyelectrolyte
383 complex consisting of chitosan as a cationic polymer and ulvan as an anionic polymer. The PEC
384 was made with a 60/40 ratio of ulvan and chitosan to form a stable gel by balancing the opposite
385 charges involved. The presence of the individual polysaccharides in the PEC scaffold was done by
386 the major bands in the infrared region, namely the band at the 1596 cm^{-1} from the amine groups and
387 a band at 1622 cm^{-1} from the carboxylates. The polysaccharide gels swell to a maximum of around
388 400% in SBF medium. This swelling potential is lower as compared to the UV crosslinked ulvan
389 scaffolds mostly due to the neutralization of charges, which lowers the uptake of water. These
390 scaffolds were further mineralized using three different concentrations of ALP as mineral inducing
391 enzyme. A higher concentration of the enzyme leads to more mineral deposits as indicated by the
392 weight change data. SEM revealed the morphology of the formed minerals as rounded aggregates
393 with a Ca:P ratio varying from 1.1 to 1.7. The XRD results also indicated that a certain
394 concentration of the enzyme is able to deposit minerals with a Ca:P ratio close to hydroxyapatite in
395 a similar polymeric matrix. Confocal laser scanning microscopy indicated that enzymatically
396 treated samples showed improved adhesion and proliferation with cubical shaped cells. Cells seeded
397 on the enzymatically-mineralized matrix formed a dense extra cellular matrix at the edge of the
398 scaffold as observed with histology. The cell proliferation, ALP activity and collagen production
399 indicate that UC 25 samples show higher activity than the UC 50 samples. As compared to the UV
400 crosslinked ulvan matrix, there is not much difference in the characteristic of the mineralized
401 scaffolds, hence it can be inferred that irrespective of the matrix property, ALP is able to induce

402 minerals and the formed minerals support cell proliferation, differentiation and matrix formation in
403 the scaffolds. However, such PEC's offer better alternative compared to UV crosslinkable ulvan as
404 a matrix since it is greener route of developing resorbable scaffolds.

405 **5. CONCLUSIONS**

406 The study was performed as a follow-up investigation of the previously published result of ulvan
407 methacrylate as a matrix for enzyme induced mineralization. A comparatively greener route was
408 followed to develop gels of ulvan. In this study ulvan and chitosan were employed to form a
409 polyelectrolyte complex and the resulting scaffolds were treated with ALP and calcium phosphate
410 minerals were successfully deposited. The PEC's were stable and could be confirmed by FTIR.
411 Mineralization on the PEC scaffolds was done using three different concentrations of ALP which
412 deposited calcium phosphate minerals with Ca:P ratio ranging from 1.2 to 1.7 which varied in
413 relation to the concentration of ALP used for mineralization. The mineralized scaffolds were non-
414 toxic and promoted cell adhesion and differentiation towards an osteogenic phenotype. The cells
415 formed a dense extracellular matrix as revealed by the histological analysis. These scaffolds could
416 successfully find application as resorbable scaffolds and can be a better alternative in some aspects
417 compared to UV crosslinked ulvan matrix.

418 **Corresponding Author**

419 *Email: mamoni.dash@niser.ac.in, mamonidash@gmail.com, (M.D)

420

421 **AUTHOR INFORMATION**

422 **Mamoni Dash, SBS, NISER**

423

424 **Notes**

425 The authors declare no competing financial interest.

426

427 **ACKNOWLEDGEMENTS**

428 M. D acknowledges the Science and Engineering Research Board (YSS/2015/001940), Department
429 of Science and Technology, Government of India. Prof. Philippe F Smet is highly acknowledged
430 and thanked for his extremely valuable input on SEM and EDX analysis. S.K.S acknowledges
431 Department of Science and Technology (DST) Ramanujan Fellowship (grant agreement No
432 SB/S2/RJN-038/2016) and Ramalingaswami Fellowship 2016-17 (D.O.NO.BT/HRD/35/02/2006).
433 H.A.D. was supported by Ghent University (Postdoctoral Grant No. BOF IV1-I/0002/03). T.E.L.D.
434 acknowledges the Research Foundation Flanders (FWO) for financial support in the framework of a
435 postdoctoral research fellowship.

436 **REFERENCES**

- 437 Costa, D. O., Dixon, S. J., & Rizkalla, A. S. (2012). One- and Three-Dimensional Growth of
438 Hydroxyapatite Nanowires during Sol–Gel–Hydrothermal Synthesis. *ACS Applied*
439 *Materials & Interfaces*, 4(3), 1490-1499.
- 440 Dash, M., Chiellini, F., Fernandez, E. G., Piras, A. M., & Chiellini, E. (2011). Statistical approach
441 to the spectroscopic determination of the deacetylation degree of chitins and chitosans.
442 *Carbohydrate Polymers*, 86(1), 65-71.
- 443 Dash, M., Chiellini, F., Ottenbrite, R. M., & Chiellini, E. (2011). Chitosan—A versatile semi-
444 synthetic polymer in biomedical applications. *Progress in Polymer Science*, 36(8), 981-
445 1014.
- 446 Dash, M., Piras, A. M., & Chiellini, F. (2009). *Chitosan-Based Beads for Controlled Release of*
447 *Proteins*. In *Hydrogels: Biological Properties and Applications* (pp. 111-120). Milano:
448 Springer Milan
- 449 Dash, M., Samal, S. K., Bartoli, C., Morelli, A., Smet, P. F., Dubruel, P., & Chiellini, F. (2014).
450 Biofunctionalization of Ulvan Scaffolds for Bone Tissue Engineering. *ACS Applied*
451 *Materials & Interfaces*, 6(5), 3211-3218.
- 452 Dash, M., Samal, S. K., Douglas, T. E. L., Schaubroeck, D., Leeuwenburgh, S. C., Van Der Voort,
453 P., . . . Dubruel, P. (2015). Enzymatically biomineralized chitosan scaffolds for tissue-
454 engineering applications. *Journal of Tissue Engineering and Regenerative Medicine*, n/a-
455 n/a.
- 456 Douglas, T. E. L., Gassling, V., Declercq, H. A., Purcz, N., Pamula, E., Haugen, H. J., . . .
457 Leeuwenburgh, S. C. G. (2012). Enzymatically induced mineralization of platelet-rich
458 fibrin. *Journal of Biomedical Materials Research Part A*, 100A(5), 1335-1346.
- 459 Douglas, T. E. L., Messersmith, P. B., Chasan, S., Mikos, A. G., de Mulder, E. L. W., Dickson, G., .
460 . . Leeuwenburgh, S. C. G. (2012). Enzymatic Mineralization of Hydrogels for Bone Tissue
461 Engineering by Incorporation of Alkaline Phosphatase. *Macromolecular Bioscience*, 12(8),
462 1077-1089.

- 463 Douglas, T. E. L., Skwarczynska, A., Modrzejewska, Z., Balcaen, L., Schaubroeck, D., Lycke, S., .
464 . . . Leeuwenburgh, S. C. G. (2013). Acceleration of gelation and promotion of mineralization
465 of chitosan hydrogels by alkaline phosphatase. *International Journal of Biological*
466 *Macromolecules*, 56, 122-132.
- 467 Douglas, T. E. L., Wlodarczyk, M., Pamula, E., Declercq, H. A., de Mulder, E. L. W., Bucko, M.
468 M., . . . Leeuwenburgh, S. C. G. (2014). Enzymatic mineralization of gellan gum hydrogel
469 for bone tissue-engineering applications and its enhancement by polydopamine. *Journal of*
470 *Tissue Engineering and Regenerative Medicine*, 8(11), 906-918.
- 471 Franceschi, R. T., & Iyer, B. S. (1992). Relationship between collagen synthesis and expression of
472 the osteoblast phenotype in MC3T3-E1 cells. *Journal of Bone and Mineral Research*, 7(2),
473 235-246.
- 474 Gassling, V., Douglas, T. E. L., Purcz, N., Schaubroeck, D., Balcaen, L., Bliznuk, V., . . . Dubruel,
475 P. (2013). Magnesium-enhanced enzymatically mineralized platelet-rich fibrin for bone
476 regeneration applications. *Biomedical Materials*, 8(5), 055001.
- 477 Gazzarri, M., Bartoli, C., Mota, C., Puppi, D., Dinucci, D., Volpi, S., & Chiellini, F. (2013). Fibrous
478 star poly(ϵ -caprolactone) melt-electrospun scaffolds for wound healing applications. *Journal*
479 *of Bioactive and Compatible Polymers*.
- 480 Habibovic, P., & de Groot, K. (2007). Osteoinductive biomaterials—properties and relevance in
481 bone repair. *Journal of Tissue Engineering and Regenerative Medicine*, 1(1), 25-32.
- 482 Junqueira, L. C. U., Bignolas, G., & Brentani, R. R. (1979). A simple and sensitive method for the
483 quantitative estimation of collagen. *Analytical Biochemistry*, 94(1), 96-99.
- 484 Koupaei, N., & Karkhaneh, A. (2016). Porous crosslinked polycaprolactone hydroxyapatite
485 networks for bone tissue engineering. *Tissue Engineering and Regenerative Medicine*,
486 13(3), 251-260.
- 487 Lawrie, G., Keen, I., Drew, B., Chandler-Temple, A., Rintoul, L., Fredericks, P., & Grøndahl, L.
488 (2007). Interactions between Alginate and Chitosan Biopolymers Characterized Using FTIR
489 and XPS. *Biomacromolecules*, 8(8), 2533-2541.
- 490 Lišková, J., Douglas, T. E. L., Beranová, J., Skwarczyńska, A., Božič, M., Samal, S. K., . . .
491 Bačáková, L. (2015). Chitosan hydrogels enriched with polyphenols: Antibacterial activity,
492 cell adhesion and growth and mineralization. *Carbohydrate Polymers*, 129, 135-142.
- 493 Lupascu, F. G., Dash, M., Samal, S. K., Dubruel, P., Lupusoru, C. E., Lupusoru, R.-V., . . . Profire,
494 L. (2015). Development, optimization and biological evaluation of chitosan scaffold
495 formulations of new xanthine derivatives for treatment of type-2 diabetes mellitus.
496 *European Journal of Pharmaceutical Sciences*, 77, 122-134.
- 497 Morelli, A., & Chiellini, F. (2010). Ulvan as a New Type of Biomaterial from Renewable
498 Resources: Functionalization and Hydrogel Preparation. *Macromolecular Chemistry and*
499 *Physics*, 211(7), 821-832.
- 500 Muzzarelli, R., Tarsi, R., Filippini, O., Giovanetti, E., Biagini, G., & Varaldo, P. E. (1990).
501 Antimicrobial properties of N-carboxybutyl chitosan. *Antimicrobial Agents and*
502 *Chemotherapy*, 34(10), 2019-2023.
- 503 Muzzarelli, R. A. A. (2011). Biomedical Exploitation of Chitin and Chitosan via Mechano-
504 Chemical Disassembly, Electrospinning, Dissolution in Imidazolium Ionic Liquids, and
505 Supercritical Drying. *Marine Drugs*, 9(9), 1510-1533.
- 506 Olivares-Navarrete, R., Lee, E. M., Smith, K., Hyzy, S. L., Doroudi, M., Williams, J. K., . . .
507 Schwartz, Z. (2017). Substrate Stiffness Controls Osteoblastic and Chondrocytic
508 Differentiation of Mesenchymal Stem Cells without Exogenous Stimuli. *PLoS ONE*, 12(1),
509 e0170312.
- 510 Phadke, A., Zhang, C., Hwang, Y., Vecchio, K., & Varghese, S. (2010). Templated Mineralization
511 of Synthetic Hydrogels for Bone-Like Composite Materials: Role of Matrix Hydrophobicity.
512 *Biomacromolecules*, 11(8), 2060-2068.

- 513 Piras, A. M., Maisetta, G., Sandreschi, S., Esin, S., Gazzarri, M., Batoni, G., & Chiellini, F. (2014).
514 Preparation, physical–chemical and biological characterization of chitosan nanoparticles
515 loaded with lysozyme. *International Journal of Biological Macromolecules*, 67, 124-131.
- 516 Rauner, N., Meuris, M., Zoric, M., & Tiller, J. C. (2017). Enzymatic mineralization generates
517 ultrastiff and tough hydrogels with tunable mechanics. *Nature*, 543(7645), 407-410.
- 518 Ruhé, P. Q., Hedberg, E. L., Padron, N. T., Spauwen, P. H. M., Jansen, J. A., & Mikos, A. G.
519 (2005). Biocompatibility and degradation of poly(DL-lactic-co-glycolic acid)/calcium
520 phosphate cement composites. *Journal of Biomedical Materials Research Part A*, 74A(4),
521 533-544.
- 522 S. K. Samal, M. D., H. A. Declercq, T. Gheysens, J. D., P. V. D. Voort, & R. Cornelissen, P. D., *
523 D. L. Kaplan. (2014). Enzymatic Mineralization of Silk Scaffolds. *Macromolecular*
524 *Bioscience*, 14(DOI: 10.1002/mabi.201300513).
- 525 Saito, M., Fujii, K., Soshi, S., & Tanaka, T. (2006). Reductions in degree of mineralization and
526 enzymatic collagen cross-links and increases in glycation-induced pentosidine in the femoral
527 neck cortex in cases of femoral neck fracture. *Osteoporosis International*, 17(7), 986-995.
- 528 Samal, S. K., Dash, M., Chiellini, F., Kaplan, D. L., & Chiellini, E. (2013). Silk microgels formed
529 by proteolytic enzyme activity. *Acta Biomaterialia*, 9(9), 8192-8199.
- 530 Samal, S. K., Dash, M., Chiellini, F., Wang, X., Chiellini, E., Declercq, H. A., & Kaplan, D. L.
531 (2014). Silk/chitosan biohybrid hydrogels and scaffolds via green technology. *RSC*
532 *Advances*, 4(96), 53547-53556.
- 533 Samal, S. K., Dash, M., Declercq, H. A., Gheysens, T., Dendooven, J., Voort, P. V. D., . . . Kaplan,
534 D. L. (2014). Enzymatic Mineralization of Silk Scaffolds. *Macromolecular Bioscience*,
535 14(7), 991-1003.
- 536 Schwarz, H.-H., Richau, K., & Paul, D. (1991). Membranes from polyelectrolyte complexes.
537 *Polymer Bulletin*, 25(1), 95-100.
- 538 Slaughter, B. V., Khurshid, S. S., Fisher, O. Z., Khademhosseini, A., & Peppas, N. A. (2009).
539 Hydrogels in Regenerative Medicine. *Advanced materials (Deerfield Beach, Fla.)*, 21(0),
540 3307-3329.
- 541 St-Pierre, J.-P., Gauthier, M., Lefebvre, L.-P., & Tabrizian, M. (2005). Three-dimensional growth
542 of differentiating MC3T3-E1 pre-osteoblasts on porous titanium scaffolds. *Biomaterials*,
543 26(35), 7319-7328.
- 544 Vo, T. N., Kasper, F. K., & Mikos, A. G. (2012). Strategies for Controlled Delivery of Growth
545 Factors and Cells for Bone Regeneration. *Advanced drug delivery reviews*, 64(12), 1292-
546 1309.
- 547 Zimmermann, K. A., LeBlanc, J. M., Sheets, K. T., Fox, R. W., & Gatenholm, P. (2011).
548 Biomimetic design of a bacterial cellulose/hydroxyapatite nanocomposite for bone healing
549 applications. *Materials Science and Engineering: C*, 31(1), 43-49.

550

551